JCI The Journal of Clinical Investigation

NKTR-255 is a polymer-conjugated IL-15 with unique mechanisms of action on T and natural killer cells

Tanya O. Robinson, … , Takahiro Miyazaki, Kimberly S. Schluns

J Clin Invest. 2021;131(19):e144365. https://doi.org/10.1172/JCI144365.

Research Article **Oncology** **Therapeutics**

NKTR-255 is a PEG conjugate of recombinant human IL-15 (rhIL-15) being examined as a potential cancer immunotherapeutic. Since IL-15 responses can be mediated by trans or cis presentation via IL-15Rα or soluble IL-15/IL-15Rα complexes, we investigated the role of IL-15Rα in driving NKTR-255 responses using defined naive and memory OVA-specific $CD8^+$ T cells (OT-I) and NK cells in mice. NKTR-255 induced a 2.5- and 2.0-fold expansion of $CD8^+$ T and NK cells, respectively, in WT mice. In adoptive transfer studies, proliferation of naive and memory WT OT-I T cells in response to NKTR-255 was not impaired in IL-15Rα$^{-/-}$ mice, suggesting trans presentation was not utilized by NKTR-255. Interestingly, naive IL-15Rα$^{-/-}$ OT-I cells had deficient responses to NKTR-255, while memory IL-15Rα$^{-/-}$ OT-I cell responses were partially impaired, suggesting that naive $CD8^+$ T cells are more dependent on cis presentation of NKTR-255 than memory $CD8^+$ T cells. In bone marrow chimera studies, IL-15Rα$^{-/-}$ and WT NK cells present in WT recipients had similar responses to NKTR-255, suggesting that cis presentation is not utilized by NK cells. NKTR-255 could form soluble complexes with IL-15Rα; binding to murine IL-15Rα generated superagonists that preferentially stimulated NK cells, showing that conversion to IL-15Rβ agonist biases the response toward NK cells. These findings highlight the ability of NKTR-255 to utilize IL-15Rα for cis presentation and act as […]

NKTR-255 is a polymer-conjugated IL-15 with unique mechanisms of action on T and natural killer cells

Tanya O. Robinson,[1] Shweta M. Hegde,[1] Allison Chang,[2] Achintyan Gangadharan,[1] Sarai Rivas,[1] Loui Madakamutil,[3] Jonathan Zalevsky,[4] Takahiro Miyazaki,[3] and Kimberly S. Schluns[1]

[1]Department of Immunology, University of Texas MD Anderson Cancer Center, Houston, Texas, USA. [2]Chemical and Biomedical Engineering, Rice University, Houston, Texas, USA. [3]Research Biology: Pharmacology, and [4]Research and Development, Nektar Therapeutics, San Francisco, California, USA.

NKTR-255 is a PEG conjugate of recombinant human IL-15 (rhIL-15) being examined as a potential cancer immunotherapeutic. Since IL-15 responses can be mediated by trans or cis presentation via IL-15Rα or soluble IL-15/IL-15Rα complexes, we investigated the role of IL-15Rα in driving NKTR-255 responses using defined naive and memory OVA-specific CD8$^+$ T cells (OT-I) and NK cells in mice. NKTR-255 induced a 2.5- and 2.0-fold expansion of CD8$^+$ T and NK cells, respectively, in WT mice. In adoptive transfer studies, proliferation of naive and memory WT OT-I T cells in response to NKTR-255 was not impaired in IL-15Rα$^{-/-}$ mice, suggesting trans presentation was not utilized by NKTR-255. Interestingly, naive IL-15Rα$^{-/-}$ OT-I cells had deficient responses to NKTR-255, while memory IL-15Rα$^{-/-}$ OT-I cell responses were partially impaired, suggesting that naive CD8$^+$ T cells are more dependent on cis presentation of NKTR-255 than memory CD8$^+$ T cells. In bone marrow chimera studies, IL-15Rα$^{-/-}$ and WT NK cells present in WT recipients had similar responses to NKTR-255, suggesting that cis presentation is not utilized by NK cells. NKTR-255 could form soluble complexes with IL-15Rα; binding to murine IL-15Rα generated superagonists that preferentially stimulated NK cells, showing that conversion to IL-15Rβ agonist biases the response toward NK cells. These findings highlight the ability of NKTR-255 to utilize IL-15Rα for cis presentation and act as an IL-15Rαβ agonist on CD8$^+$ T cells.

Introduction

IL-15 is a cytokine expressed in the steady state that has crucial functions in lymphocyte development and homeostasis. Specifically, in mice, IL-15 drives NK cell development and the generation of memory CD8$^+$ T cells. Once memory CD8$^+$ T cells differentiate, IL-15 helps maintain memory CD8$^+$ T cell numbers by promoting homeostatic proliferation (1, 2). IL-15 also maintains NK cell numbers by promoting survival (3). While these functions are mediated by constitutively expressed IL-15, IL-15 has additional functions when upregulated or when given exogenously. IL-15 promotes activation and proliferation of naive and memory CD8$^+$ T cells in the absence of overt antigen stimulation and enhances IFN-γ and granzyme B production by effector CD8$^+$ T cells and NK cells (4–7). Thus, the preferential stimulation of CD8$^+$ T cells and NK cells by IL-15 makes it an attractive cytokine for use in cancer immunotherapy. Indeed, studies have demonstrated that exogenous systemic delivery of recombinant human IL-15 (rhIL-15) enhances antitumor responses in a number of preclinical mouse models and in human trials (8). Furthermore, the antitumor effects of IL-15 overlap with those of IL-2, as both cytokines signal through the shared IL-2/IL-15 receptor β (CD122) and the common γ_c (CD132) receptors. While IL-15 and IL-2 enhance the functions of CD8$^+$ T cells and NK cells, IL-15 has an added advantage over IL-2 in that it does not stimulate regulatory CD4$^+$ T cells. However, IL-15 differs significantly from IL-2 in its very short in vivo half-life, thus limiting its efficacy (9).

Studies have provided evidence that rhIL-15 does not mimic endogenous IL-15, which contributes to its weak in vivo efficacy (10, 11). Additionally, there are multiple possible mechanisms by which IL-15 can stimulate responses in vivo. IL-15 is coexpressed with IL-15Rα, which binds intracellularly and is shuttled to the cell surface (10). Thus, IL-15Rα does not act as a conventional cytokine receptor, but rather as a chaperone protein. The coexpression of IL-15 and IL-15Rα along with the high affinity of IL-15Rα for IL-15 (1.4×10^{-11} M) (12, 13) prevents unbound or free IL-15 from being expressed in physiological settings (11). Furthermore, IL-15Rα protein expression likely exceeds that of IL-15, as IL-15Rα is readily detected on a wide range of cell types, while cell-surface–associated IL-15 is difficult to detect (14). Cell-surface IL-15Rα/IL-15 complexes are thought to stimulate opposing cells via a mechanism called trans presentation, which is believed to be the major mechanism driving lymphocyte development and homeostasis (15). Soluble IL-15 (sIL-15)/IL-15Rα complexes are also found in the serum of normal mice and are increased by a variety of inflammatory stimuli (11, 16, 17). The presence of sIL-15 complexes is due to natural shedding as well as cleavage by cell-surface metalloproteases, which are activated by inflammatory signals (18). Patients subjected to lymphodepleting chemotherapy also have elevated levels of sIL-15 complexes (11). Elevated levels of sIL-15 complexes correlate with enhanced IL-15 responses; however, the role of endogenously

Conflict of interest: TM and LM report coinventorship on patent EP3876974A1 (Long-acting interleukin-15 receptor agonist in combination with another pharmacologically active agent), licensed to Nektar Therapeutics.

Submitted: September 29, 2020; **Accepted:** August 6, 2021; **Published:** October 1, 2021.
Reference information: *J Clin Invest*. 2021;131(19):e144365.
https://doi.org/10.1172/JCI144365.

produced sIL-15 complexes is still not clearly established. Because IL-15–responsive cells, including $CD8^+$ T cells and NK cells, express IL-15Rα (14), IL-15Rα also has the potential to deliver IL-15 to the IL-2/15Rβ/γ_c receptor on the same cell via cis presentation. While evidence suggests that cis presentation is not a major mechanism driving endogenous IL-15 responses, cis presentation could be active when free rhIL-15 is delivered therapeutically.

Although alternative rhIL-15–based agonists, including an Fc-fusion protein, have been developed to improve pharmacokinetic (PK) profiles, unexpectedly, they still show high rates of systemic elimination (19). Polymer conjugation is a well-validated approach to altering and optimizing the biological properties of macromolecules. PEG chains can be designed to modify not only a molecule's PK, but also its receptor-binding properties (20). Bempegaldesleukin (BEMPEG or NKTR-214) was designed to improve the half-life, PK, pharmacodynamics (PD), efficacy, and tolerability of IL-2 by using PEGylation technology. It is currently the most advanced IL-2 pathway–targeted agent in clinical development for oncology, with multiple active registrational phase III studies (21). Nektar Therapeutics has engineered the PEG conjugate of rhIL-15, called NKTR-255, that was designed to exhibit sustained PD and enhanced in vivo efficacy with an improved PK profile over rhIL-15 (22). We sought to identify the mechanisms by which NKTR-255 mediates IL-15 responses and determine how they dictate cell-specific responses. Since rhIL-15 is biologically active in mice, we were able to dissect the cellular requirements of NKTR-255 for IL-15Rα.

Results

NKTR-255 induces expansion of $CD8^+$ T cells and NK cells. To measure the extent to which NKTR-255 stimulates various lymphocyte subsets, mice were treated with a single dose of NKTR-255 and the total numbers of NK, $CD8^+$, and $CD4^+$ cells were quantitated 5 days later. We chose to deliver only one dose and examine $CD4^+$ and $CD8^+$ cells and NK cells for a short time frame to visualize responses by treatment-naive lymphocytes and limit conversion to a more IL-15–responsive subset. In response to NKTR-255, splenic NK cells significantly increased in frequency and total NK cell numbers almost 2-fold (Figure 1, A and B). $CD4^+$ T cell frequencies and total numbers were not significantly affected by NKTR-255 treatment. The frequency of $CD8^+$ T cells in the spleen increased from 10% to 16%, which constituted a 2.5-fold increase in total $CD8^+$ T cells (Figure 1, A and B). The increase in $CD8^+$ T cells preferentially affected the $CD44^{hi}$ population (Figure 1, C and D). Among the $CD44^{hi}$ $CD8^+$ T cells, the number of cells increased 4.5-fold in the $CD62L^+$ subset compared with 2.5-fold in the $CD62L^-$ subset (Figure 1E). The increases in $CD8^+$ T cells and NK cells induced by NKTR-255 were due to a greater induction of proliferation, as BrdU incorporation increased among NK cells and $CD44^{hi}$ $CD8^+$ T cells (Figure 1F).

To determine whether NKTR-255 responses were similar in C57BL/6 and BALB/c mice, age- and sex-matched mice from both backgrounds were treated with NKTR-255 and frequency and changes in lymphocyte populations were examined. In untreated mice, the frequency of NK cells was lower for C57BL/6 mice than BALB/c mice (Supplemental Figure 1, A and B; supplemental material available online with this article; https://doi.org/10.1172/JCI144365DS1). Moreover, NK cells in BALB/c mice responded better to NKTR-255 than NK cells in C57BL/6 mice, as demonstrated by a 2.4-fold increase in the total numbers in the spleens of C57BL/6 mice and a corresponding 4.3-fold increase in BALB/c mice (Supplemental Figure 1, A and B). In contrast, the expansion of $CD44^{hi}$ $CD8^+$ T cells in response to NKTR-255 was greater in C57BL/6 mice than in BALB/c mice (Supplemental Figure 1, A and B). CD122 expression among lymphocyte populations was not different between C57BL/6 and BALB/c mice (data not shown). The differences observed predict that NKTR-255 could mediate slightly different responses in these 2 strains of mice, depending on the requirement for $CD8^+$ T cells versus NK cells.

Since IL-15 promotes NK cell maturation (19), we examined the effects of NKTR-255 on this process. During NK cell development, NK cell maturation can be divided into 3 stages in which cells transition from immature ($CD11b^-CD27^+$) to the mature stage 1 ($CD11b^+CD27^+$) and finally the mature stage 2 ($CD11b^+CD27^-$). Compared with those in untreated mice, NK cells in NKTR-255–treated mice had a decreased proportion of stage 1 mature cells and an increased frequency of stage 2 mature cells in both spleen and bone marrow (BM) (Figure 2, A and B). In the analysis of total cell numbers, NK cells in each stage increased in response to NKTR-255, with the most mature subset, the $CD11b^+CD27^-$ population, exhibiting the largest fold increase (Figure 2B).

NKTR-255 binds IL-15Rα and fails to induce a response in the absence of IL-15Rα expression. To determine whether NKTR-255 binds to cell-surface IL-15Rα in vivo, we treated WT C57BL/6 mice with NKTR-255 and determined whether we could detect NKTR-255 binding using $CD11c^+$ splenocytes stained for human IL-15 (hIL-15) using immunofluorescent staining. $CD11c^{hi}$ splenocytes were analyzed, as they have been shown to express high levels of IL-15Rα and are a major cell type trans presenting IL-15 (14). We also utilized transgenic (Tg) mice expressing IL-15Rα under the CD11c promoter (CD11c–IL-15Rα Tg), which have been previously described (14). In WT mice, we could not detect a significant level of NKTR-255 binding by $CD11c^{hi}$ splenocytes or on any other splenic myeloid cells, as detected by anti–hIL-15 Ab (Figure 3A). However, in NKTR-255–treated CD11c–IL-15Rα Tg mice, NKTR-255 could be detected on $CD11c^{hi}$ cells in a pattern mimicking Tg IL-15Rα expression (Figure 3A). Similar findings were observed with in vitro incubation of NKTR-255 with splenocytes isolated from CD11c–IL-15Rα Tg mice (Figure 3B). Furthermore, in vitro incubation with recombinant murine IL-15 (rmIL-15) could block binding of NKTR-255 (Figure 3B). Overall, these results indicated that NKTR-255 binds cell-surface IL-15Rα and thus has the potential to be trans presented.

To determine whether NKTR-255 responses are dependent on IL-15Rα, IL-15Rα$^{-/-}$ mice were treated with NKTR-255, as described above, and changes in T cells and NK cells were assessed. The frequency and total number of NK cells, $CD8^+$ T cells, and $CD4^+$ T cells were unaffected by NKTR-255 treatment in IL-15Rα$^{-/-}$ mice (Figure 3C). These findings suggested that NKTR-255 responses are dependent on IL-15Rα; however, a caveat of analyzing IL-15Rα$^{-/-}$ mice is their deficiency in IL-15–responding lymphocytes. This was addressed in later experiments.

Responses induced by NKTR-255 do not require trans presentation. Previous studies provided evidence that IL-15 bound to IL-15Rα on the cell surface is trans presented to IL-15–responsive

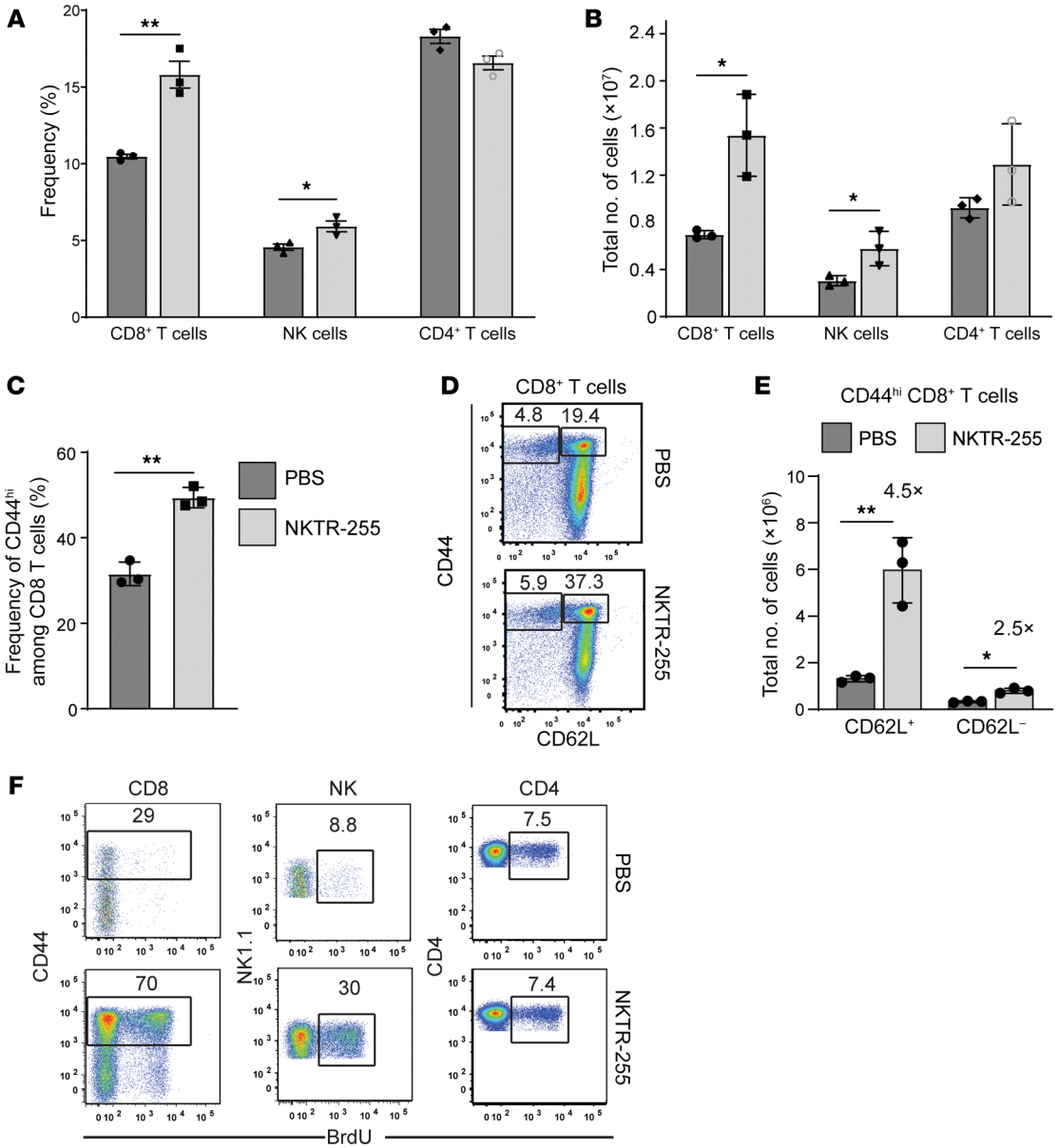

Figure 1. NKTR-255 increases CD8⁺ T cells and NK cells. C57BL/6 mice (n = 3/group) were treated with NKTR-255 (0.03 mg/kg, i.p). Five days after treatment, splenocytes were harvested and analyzed by flow cytometry. (**A** and **B**) Mean frequency and total numbers of CD8⁺ T cells, NK cells, and CD4⁺ T cells. (**C**) Average frequency of CD44^{hi} CD8⁺ T cells. (**D**) CD62L and CD44 expression by CD8⁺ T cells. (**E**) Total numbers of CD62L⁺ and CD62L⁻ CD44^{hi} CD8⁺ T cells in spleens of PBS- and NKTR-255–treated mice. Numbers above bars indicate average fold increase in total cell numbers. (**F**) In separate experiments, NKTR-255– and PBS-treated mice (n = 3–5/group) were given BrdU (2 mg, i.p.) every 2 days and analyzed 5 days later. Representative flow cytometry plots show BrdU incorporation by CD8⁺ T cells, NK cells, and CD4⁺ T cells. Error bars represent SD. Similar results were observed in at least 2 additional experiments. *P < 0.05; **P < 0.01, 2-tailed Student's t test.

cells in a cell–cell interaction (10, 22, 23). We determined whether NKTR-255 was similarly trans presented to IL-15–responsive cells in vivo. Naive OVA-specific CD8⁺ (OT-I) T cell receptor (TCR) Tg CD8⁺ T cells (RAG$^{-/-}$, CD45.1) were labeled with CFSE and transferred into congenic WT or IL-15Rα$^{-/-}$ mice (CD45.2⁺), which was followed by treatment with NKTR-255. Naive T cells proliferated in response to NKTR-255 in IL-15Rα$^{-/-}$ recipients as well as in WT recipients, suggesting IL-15Rα expression by host cells was not critical (Figure 4, A and B). In an analysis of phenotypic changes that occur with NKTR-255 treatment, naive T cells that had proliferated in response to NKTR-255 upregulated CD44 and maintained CD62L expression, demonstrating a conversion to a central memory phenotype (Figure 4A). Therefore, the conversion of naive T cells to CD62L⁺CD44^{hi} CD8⁺ T cells contributed partially to the increase in this subset following NKTR-255 treatment. Moreover, the extent of proliferation among OT-I T cells was similar among spleen and peripheral lymph nodes (pLNs) and somewhat higher in BM (Figure 4C).

To investigate whether memory CD8⁺ T cell responses to NKTR-255 also lack a requirement for IL-15Rα by the recipient,

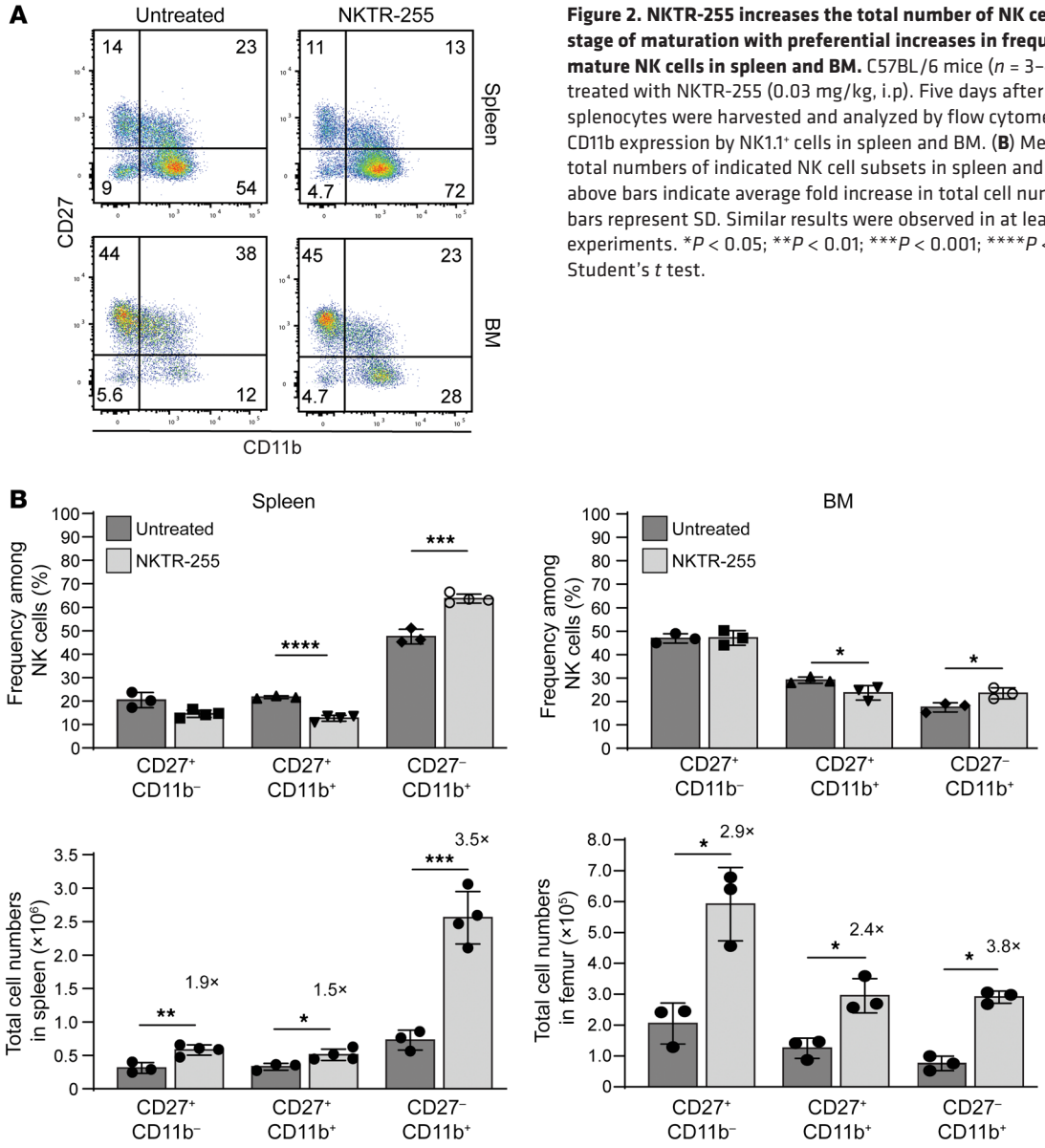

Figure 2. NKTR-255 increases the total number of NK cells at each stage of maturation with preferential increases in frequency of stage 2 mature NK cells in spleen and BM. C57BL/6 mice (n = 3–4/group) were treated with NKTR-255 (0.03 mg/kg, i.p). Five days after treatment, splenocytes were harvested and analyzed by flow cytometry. (**A**) CD27 and CD11b expression by NK1.1$^+$ cells in spleen and BM. (**B**) Mean frequency and total numbers of indicated NK cell subsets in spleen and BM. Numbers above bars indicate average fold increase in total cell numbers. Error bars represent SD. Similar results were observed in at least 2 additional experiments. *P < 0.05; **P < 0.01; ***P < 0.001; ****P < 0.0001, 2-tailed Student's t test.

memory OT-I T cells were first generated by transferring naive CD8$^+$ T cells into WT mice, followed by infection with vesicular stomatitis virus-expressing OVA (VSV-OVA). Then, at least 30 days after infection, total CD8$^+$ T cells containing memory OT-I T cells were enriched, CFSE labeled, transferred into WT and IL-15Rα$^{-/-}$ recipients, and treated with NKTR-255. Consistent with the effects observed with naive OT-I T cells, memory OT-I T cells proliferated in a similar manner in both WT and IL-15Rα$^{-/-}$ recipients (Figure 4, D and E). Additionally, among the memory OT-I T cells, the proportion of CD62L$^+$ and CD62L$^-$ subsets did not change with NKTR-255 treatment and the extent of proliferation by each subset in response to NKTR-255 was the same (Figure 4D). This finding suggested that, among an established antigen-specific memory CD8$^+$ T cell population, the CD62L$^+$ memory T cells did not preferentially increase compared with CD62L$^-$ memory T cells. Since NKTR-255 does not appear to utilize trans presentation as murine IL-15 (mIL-15) does, we determined whether rhIL-15 was trans presented to memory CD8$^+$ T cells. Unlike in our observations with NKTR-255, established memory OT-I T cells did not respond to rhIL-15 in IL-15Rα$^{-/-}$ recipients, but did respond in WT recipients (Supplemental Figure 2, A and B), indicating that hIL-15 was trans presented to memory CD8$^+$ T cells similarly to mIL-15. Moreover, this suggested that the specific polymer conjugation of NKTR-255 alters its ability to be trans presented to memory CD8$^+$ T cells. Overall, trans presentation of NKTR-255 was not required for naive or memory OT-I T cell responses.

Cis presentation of NKTR-255 is important for responses by CD8$^+$ T cells, but not NK cells. We next investigated whether IL-15Rα expression by CD8$^+$ T cells is important for NKTR-255 responses. We compared responses of OT-I T cells on the WT background (CD45.1) to OT-I T cells bred to the IL-15Rα$^{-/-}$ background (CD45.1/CD45.2). WT and IL-15Rα$^{-/-}$ OT-I T cells were mixed at a 1:1 ratio, CFSE labeled, and transferred into congenic WT recipient mice, followed by treatment with NKTR-255. WT OT-I T cells proliferated more extensively in response to NKTR-255 than IL-15Rα$^{-/-}$ OT-I T cells (Figure 5, A and B), suggesting that NKTR-

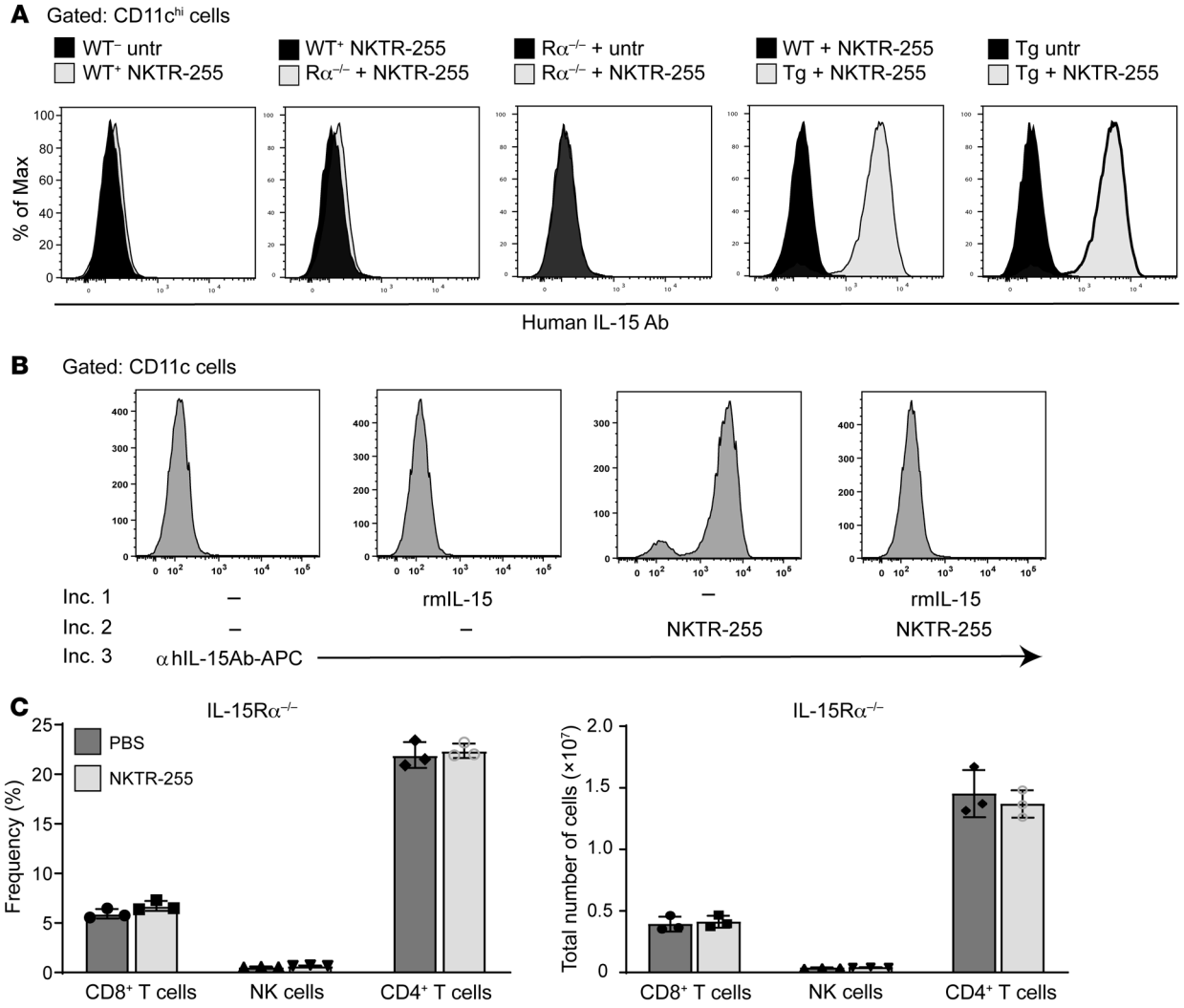

Figure 3. NKTR-255 requires IL-15Rα. (**A**) Cell-surface staining for hIL-15 by CD11c^{hi} cells in spleens of indicated mice treated with NKTR-255 one day earlier. (**B**) Splenocytes from untreated CD11c–IL-15Rα Tg mice were preincubated with NKTR-255 or rmIL-15 followed by staining for hIL-15. Histograms show hIL-15 staining after gating on CD11c^{hi} cells. (**C**) Frequency and total cell numbers of lymphocyte populations in spleens of IL-15Rα$^{-/-}$ mice treated 5 days earlier with NKTR-255 (0.03 mg/kg, i.p.) or PBS. Error bars represent SD. *n* = 3/group. Similar results were observed in an additional experiment. untr, untreated; inc, incubation.

255 utilizes IL-15Rα expressed by naive CD8$^+$ T cells, possibly through cis presentation. This requirement for IL-15Rα by naive CD8$^+$ T cells was not observed upon treatment with rhIL-15/sIL-15Rα-Fc complexes or multiple doses of rhIL-15, thereby validating that IL-15Rα$^{-/-}$ OT-I T cells were not defective in their general ability to respond to IL-15 (Figure 5, A and B, and Supplemental Figure 2, C and D). Furthermore, these findings demonstrated that NKTR-255 utilized mechanisms that were somewhat different from those of rhIL-15 or sIL-15 complexes.

We also investigated the requirements for IL-15Rα by bona fide memory CD8$^+$ T cells in response to NKTR-255. To establish memory CD8$^+$ T cells, naive WT and IL-15Rα$^{-/-}$ OT-I T cells were transferred separately into a cohort of congenic WT mice followed by infection with VSV-OVA. At least 1 month later, CD8$^+$ T cells (containing memory OT-I T cells) were enriched, CFSE labeled, transferred into a second cohort of congenic WT mice, and treated with NKTR-255. One week later, both WT and IL-15Rα$^{-/-}$ memory CD8$^+$ T cells proliferated in response to NKTR-255; however, WT memory CD8$^+$ T cells consistently proliferated to a greater extent than IL-15Rα$^{-/-}$ memory CD8$^+$ T cells (Figure 5, C and D). Therefore, expression of IL-15Rα by memory CD8$^+$ T cells was not absolutely necessary for NKTR-255 responses, but made them more responsive to NKTR-255.

Our findings that IL-15Rα$^{-/-}$ memory CD8$^+$ T cells respond to NKTR-255 in WT recipients and that IL-15Rα expression by the recipient is not required suggested that NKTR-255 should be able to induce responses in IL-15Rα$^{-/-}$ mice. One reason IL-15Rα$^{-/-}$ mice may not have responded to NKTR-255 is that these mice lack the lymphocyte subsets that are the most responsive to IL-15, for example, NK cells and memory phenotype CD8$^+$ T cells, which express high levels of CD122 (23). To test this, we examined the response to NKTR-255 by established IL-15Rα$^{-/-}$ memory CD8$^+$ T cells in IL-15Rα$^{-/-}$ recipients. This required that we first generate a population of IL-15Rα$^{-/-}$ memory CD8$^+$ T cells in IL-15Rα$^{-/-}$ mice

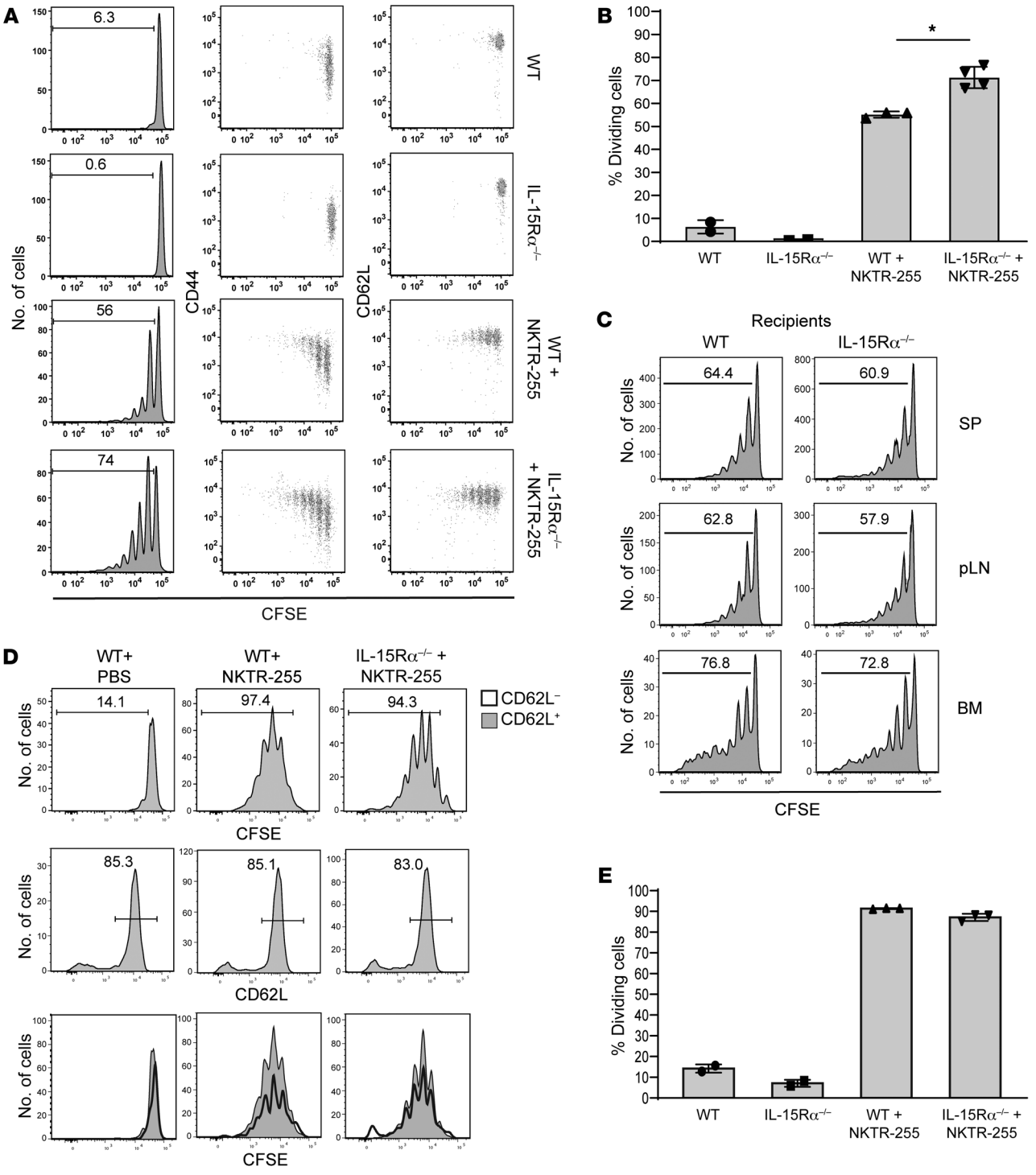

Figure 4. Responses to NKTR-255 are not dependent on trans presentation by IL-15Rα. CFSE-labeled naive OT-I T cells (CD45.1$^+$) were transferred into CD45.2$^+$ WT or IL-15Rα$^{-/-}$ mice (n = 2–4/group). One day after transfer, mice were treated with NKTR-255 (0.03 mg/kg, i.p.). Seven days later, donor CD45.1$^+$ T cells in spleens were analyzed by flow cytometry. (**A**) Representative CFSE intensity and CD44 and CD64L expression by donor T cells. (**B**) Average frequency of dividing cells ± SD (n = 3/group). (**C**) Representative CFSE dilution by naive OT-I T cells in spleen, pLNs, and BM after transfer into WT or IL-15Rα$^{-/-}$ recipients and treatment with NKTR-255 in a separate experiment from that in **A**. (**D** and **E**) CFSE-labeled CD8$^+$ T cells containing memory OT-I T cells (CD45.1$^+$) were transferred into CD45.2$^+$ WT or IL-15Rα$^{-/-}$ mice. One day later, mice were treated with NKTR-255 (0.03 mg/kg i.p.). Seven days after treatment, CFSE dilution by CD45.1$^+$ memory OT-I T cells in splenocytes was analyzed. (**D**) CFSE dilution by memory OT-I T cells (top row; bars indicate cells that have diluted CFSE), CD62L expression by memory OT-I T cells (middle row), CFSE dilution of CD62L$^-$ memory OT-I T cells (bold outline) overlaid with CD62L$^+$ OT-I T cells (shaded, thin outline; bottom row). (**E**) Average frequency of dividing cells ± SD (n = 3/group). *P < 0.05, 2-tailed Student's t test. Similar results were observed in at least 2 additional experiments. SP, spleen.

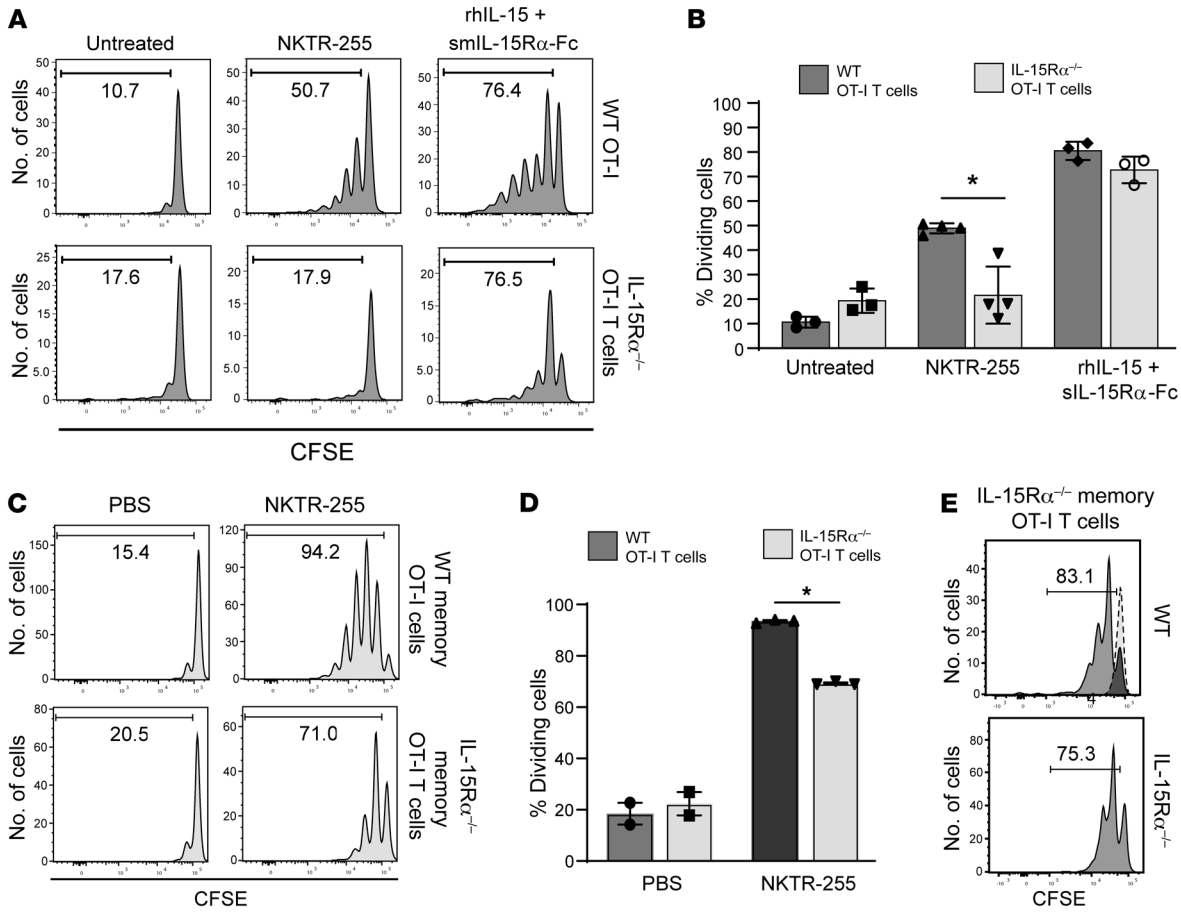

Figure 5. IL-15Rα$^{-/-}$ CD8$^+$ T cells have impaired responses to NKTR-255. CFSE-labeled naive WT (CD45.1$^+$) and IL-15Rα$^{-/-}$ (CD45.1/CD45.2$^+$) OT-I T cells (mixed at 1:1 ratio) were transferred into CD45.2$^+$ WT mice (n = 3–4/group). Seven days after transfer, mice were treated with NKTR-255 (0.03 mg/kg, i.p.) or precomplexed rhIL-15/smIL-15Rα-Fc (0.5 μg/3 μg, i.p.). (**A**) Representative CFSE intensity. (**B**) Average frequency of dividing WT (CD45.1$^+$) and IL-15Rα$^{-/-}$ (CD45.1/CD45.2$^+$) OT-I T cells ± SD (n = 3-4/group) depicted in **A**. (**C** and **D**) CFSE-labeled CD8$^+$ T cells containing WT or IL-15Rα$^{-/-}$ memory OT-I T cells (CD45.1$^+$) were transferred into CD45.2$^+$ WT or IL-15Rα$^{-/-}$ mice and treated with NKTR-255 (0.03 mg/kg i.p.) 1 day later. Seven days after treatment, CFSE dilution in CD45.1$^+$ memory OT-I T cells in splenocytes was analyzed. (**C**) CFSE dilution in CD45.1$^+$ donor T cells. (**D**) Average frequency of dividing cells ± SD (n = 2–3/group). Similar results were observed in at least 2 additional experiments. (**E**) IL-15Rα$^{-/-}$ memory OT-I T cells were generated in IL-15Rα$^{-/-}$ mice after transfer and infection with VSV-OVA. At least 30 days later, CD8$^+$ T cells were enriched, CFSE labeled, transferred into WT or IL-15Rα$^{-/-}$ recipients (~3–4 × 10^6 cells/mouse), and treated with NKTR-255 or PBS. Histograms show CFSE dilution in CD45.1$^+$ CD8$^+$ T cells (IL-15Rα$^{-/-}$ memory OT-I T cells) of NKTR-255–treated WT and IL-15Rα$^{-/-}$ recipients. Histogram overlay (dashed line) represents CFSE profile of cells in PBS-treated mice. *P < 0.05, 2-tailed Student's t test.

by transferring IL-15Rα$^{-/-}$ naive OT-I T cells into IL-15Rα$^{-/-}$ recipients followed by infection with VSV-OVA 1 day later. At least 30 days after infection, an observable population of IL-15Rα$^{-/-}$ memory OT-I CD8$^+$ T cells was present. Second, total CD8$^+$ T cells (containing IL-15Rα$^{-/-}$ memory OT-I T cells) were isolated from this cohort, CFSE labeled, and transferred to either IL-15Rα$^{-/-}$ or WT mice and treated with NKTR-255. While IL-15Rα$^{-/-}$ memory CD8$^+$ T cells responded to NKTR-255 in WT mice, they also responded to NKTR-255 in IL-15Rα$^{-/-}$ recipients (Figure 5E). Overall, these findings clearly showed that NKTR-255 responses can occur in the complete absence of IL-15Rα if IL-15–responsive lymphocytes are present.

To address whether NK cells require self-expression of IL-15Rα for responses to NKTR-255, BM chimeras were generated to allow the development of IL-15Rα$^{-/-}$ NK cells. In brief, 2 sets of BM chimeras were generated through the transfer of WT or IL-15Rα$^{-/-}$ BM cells (CD45.2$^+$) into lethally irradiated, congenic WT recipients. After the hematopoietic compartment was reconstituted, BM chimeras were treated with NKTR-255 in the presence of BrdU. One week later, BrdU incorporation by donor and host NK cells was analyzed as were changes in frequencies in lymphocyte populations. Although NK cells derived from IL-15Rα$^{-/-}$ BM were present at low frequencies, these cells still expanded in response to NKTR-255 (Supplemental Figure 3). Additionally, IL-15Rα$^{-/-}$ NK cells incorporated levels of BrdU in response to NKTR-255 that were similar to those of NK cells derived from WT BM and residual, recipient WT NK cells that survived total body irradiation (Figure 6, A and B). Overall, these data suggest that expression of IL-15Rα by NK cells was not utilized for responses to NKTR-255.

sIL-15Rα inhibits NKTR-255 responses. There have been reports that sIL-15Rα is present in the serum of human patients, which can affect antitumor responses (18, 24). We also observed that free sIL-15Rα is present in the serum of normal untreated WT mice but not IL-15Rα$^{-/-}$ mice, as detected by ELISA (Figure

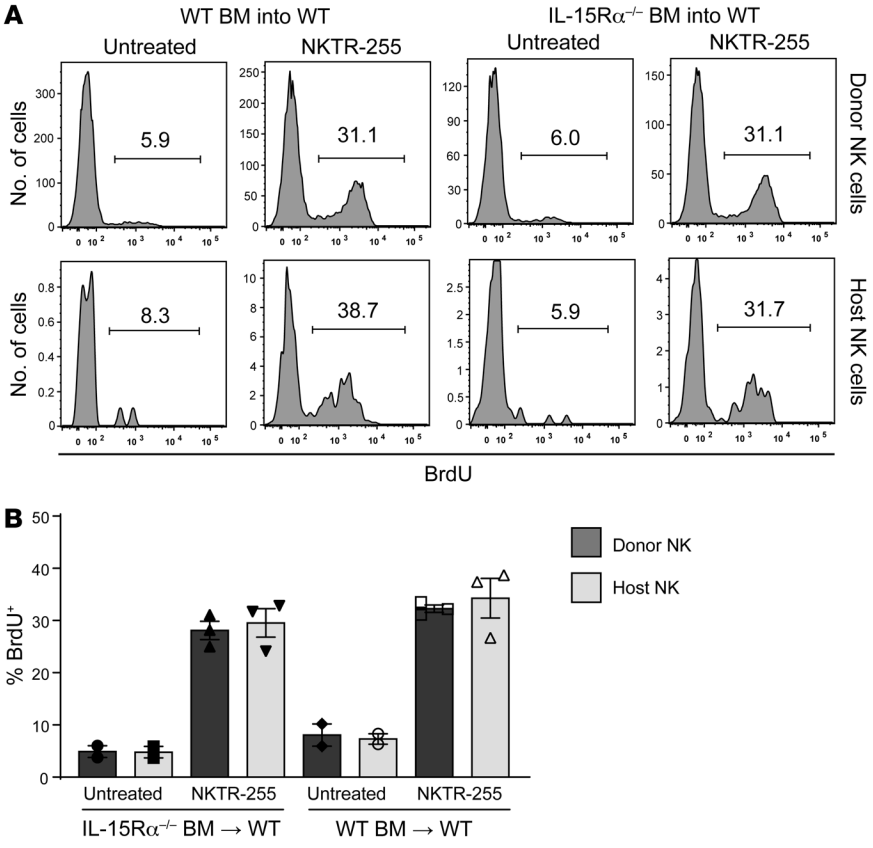

Figure 6. IL-15Rα$^{-/-}$ BM-derived NK cells incorporated levels of BrdU in response to NKTR-255 similar to those of WT BM-derived NK cells. Established IL-15Rα$^{-/-}$ BM chimeras (IL-15Rα$^{-/-}$ BM into WT) or WT BM chimeras (WT BM into WT) were treated with NKTR-255 (0.03 mg/kg, i.p.). Both treated and untreated mice (n = 3/group) were given BrdU (2 mg, i.p.) every 2 days. Five days after NKTR-255 treatment, BrdU incorporation was analyzed in splenic NK cells by flow cytometry. (**A**) BrdU incorporation after gating on CD45.2$^+$ donor-derived or CD45.1$^+$ host-derived NK1.1$^+$ cells. (**B**) BrdU incorporation ± SD. Similar results were observed in an additional experiment.

7A). In untreated WT mice in this study, the levels of sIL-15Rα (~100–200 pg/ml) were higher than the levels of sIL-15/IL-15Rα complexes (~5–10 pg/ml) previously reported (25), indicating that sIL-15Rα is produced in excess of IL-15; similar findings have been observed with regard to cell-surface IL-15Rα and IL-15 (14). In our prior studies, we generated Tg mice that had mIL-15Rα driven by the Villin promoter, and this line was maintained on the IL-15Rα$^{-/-}$ background such that IL-15Rα was expressed only in the intestinal epithelium (26). These mice exhibited an immune phenotype that resembled that of IL-15Rα$^{-/-}$ mice, but with restored populations of IL-15–dependent intestinal intraepithelial lymphocytes (26). In our present analyses, we found that these mice expressed high levels of sIL-15Rα in the serum (Figure 7A). Since these mice lack cell-surface IL-15Rα in the secondary lymphoid tissues, we set out to determine whether sIL-15Rα in the absence of cell-surface IL-15Rα affected responses to NKTR-255. In addition, Villin–IL-15Rα Tg mice backcrossed to the WT background were used to determine whether excess sIL-15Rα was inhibitory in the presence of cell-surface IL-15Rα; these mice also expressed elevated levels of sIL-15Rα in the serum compared with WT mice (Figure 7A). To this end, CFSE-labeled naive OT-I T cells were transferred into IL-15Rα$^{-/-}$, Villin-IL-15Rα Tg (IL-15Rα$^{-/-}$), WT, and Villin-IL-15Rα Tg (WT) recipients, treated with NKTR-255, and analyzed as previously described. OT-I T cell responses to NKTR-255 were impaired in Villin–IL-15Rα Tg (IL-15Rα$^{-/-}$) and Villin–IL-15Rα Tg (WT) mice compared with IL-15Rα$^{-/-}$ and WT recipients, respectively (Figure 7, B and C). Since the level of inhibition was similar in WT and IL-15Rα$^{-/-}$ backgrounds, this indicated that cell-surface IL-15Rα had little influence on responses to NKTR-255, while the presence of sIL-15Rα had a profound inhibitory effect.

To determine whether memory CD8$^+$ T cells are affected by excess sIL-15Rα, mice with established memory OT-I T cells were enriched for CD8$^+$ T cells, which were CFSE labeled and transferred into WT mice and Villin–IL-15Rα Tg (WT) mice following treatment with NKTR-255. While most memory OT-I T cells had divided in both recipients, proliferation was slower in the Villin–IL-15Rα Tg (WT) mice (Figure 7D). In these mice, NK cell expansion was also inhibited in the presence of excess sIL-15Rα in the spleen and the BM, suggesting that NK cells were also susceptible to suppression by sIL-15Rα (Figure 7, E and F). Overall, excess sIL-15Rα impaired responses to NKTR-255 by the 3 major IL-15–responsive lymphocyte populations.

NKTR-255 forms superagonists upon complexing with mIL-15Rα–Fc, but is inhibited by binding to rhIL-15Rα–Fc. Since previous studies have shown that rhIL-15 binding to rmIL-15Rα–Fc generates IL-15 super agonists (27, 28), we investigated how mixing NKTR-255 with rmIL-15Rα–Fc affects its in vivo activity. To examine this, endogenous IL-15Rα–dependent receptor-binding cytokines (NKTR-255 or rhIL-15) were incubated with rmIL-15Rα–Fc prior to injection into WT mice; the same quantity of unassociated NKTR-255 or rhIL-15 (0.6 μg/mouse) was injected into 2 additional cohorts of WT mice. Changes in the frequency of CD8$^+$ T cells, CD4$^+$ T cells, and NK cells were examined in each treatment group. Additionally, prior to treatment, WT mice were adoptively transferred with CFSE-labeled naive OT-I T cells to serve as an additional indicator of CD8$^+$ T cell proliferation. Preincubating NKTR-255 with rmIL-15Rα-Fc led to much greater expansion of

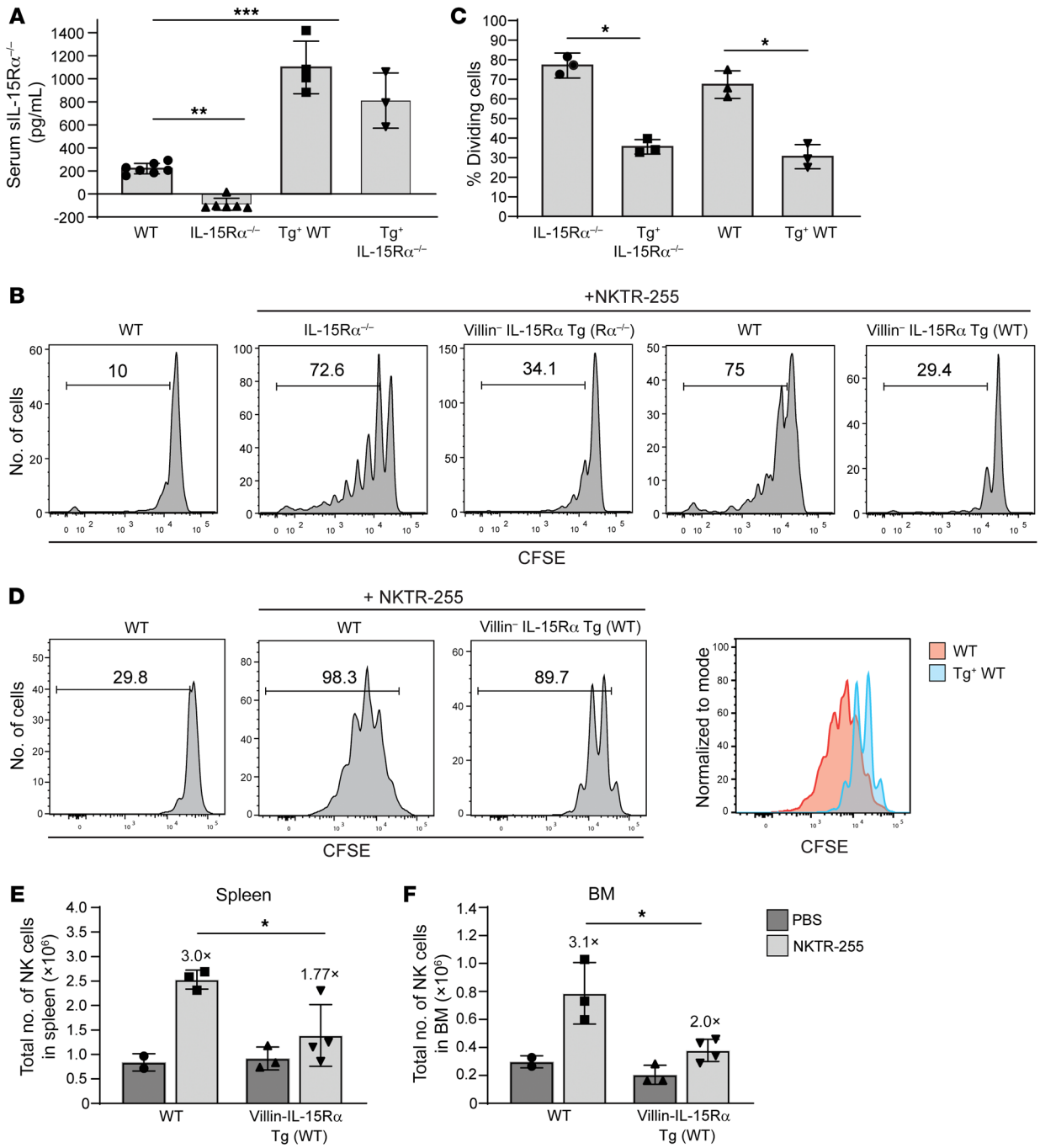

Figure 7. smIL-15Rα inhibits responses by NKTR-255. (**A**) smIL-15Rα in the serum of untreated WT, IL-15Rα$^{-/-}$, Villin–IL-15Rα Tg (IL-15Rα$^{-/-}$), and Villin–IL-15Rα Tg (WT) mice, as determined by ELISA. (**B**) CFSE-labeled CD45.1^{+} OT-I T cells were transferred into CD45.2^{+} WT, IL-15Rα$^{-/-}$, Villin–IL-15Rα Tg (IL-15Rα$^{-/-}$), or Villin–IL-15Rα Tg (WT) mice (n = 3–4/group). One day after transfer, mice were treated with NKTR-255 (0.03 mg/kg, i.p.). Six days later, splenocytes were harvested. Histograms show CFSE dilution in CD45.1^{+} donor T cells. (**C**) Bar graph shows percentage dividing OT-I T cells in IL-15Rα$^{-/-}$, Tg^{+} IL-15Rα$^{-/-}$, WT, and Tg^{+} WT mice treated with NKTR-255. Bar graph shows mean ± SD. (**D**) Representative CFSE dilution of memory OT-I T cells in WT and Villin-Tg (WT) recipients. (**E** and **F**) Graphs show total numbers of NK cells in spleens (**E**) and BM (**F**) in WT and Villin Tg^{+} (WT) after treatment with NKTR-255. Numbers above bars indicate relative fold increase in NKTR-255–treated over PBS-treated mice. *P < 0.05; **P <0.01; ***P < 0.001, 1-way ANOVA and 2-tailed Student's t test. Similar results were observed in at least 2 additional experiments.

NK cells and CD44^{hi} CD8^{+} T cells compared with unassociated NKTR-255 (Figure 8A). As previously shown, rhIL-15 (at this dose) had no effect on IL-15–responsive lymphocytes due to its very short in vivo half-life. Naive OT-I T cells also had an enhanced response to complexed NKTR-255 compared with unassociated NKTR-255, which was similar to that observed with IL-15Rα–independent (precomplexed rhIL-15/IL-15Rα-Fc) cytokines (Figure 8, B and C). Interestingly, while NKTR-255/rmIL-15Rα–Fc complexes and rhIL-15/rmIL-15Rα–Fc complexes had a similar effect on the expansion of CD8^{+} T cells, NKTR-255/rmIL-15Rα–Fc was

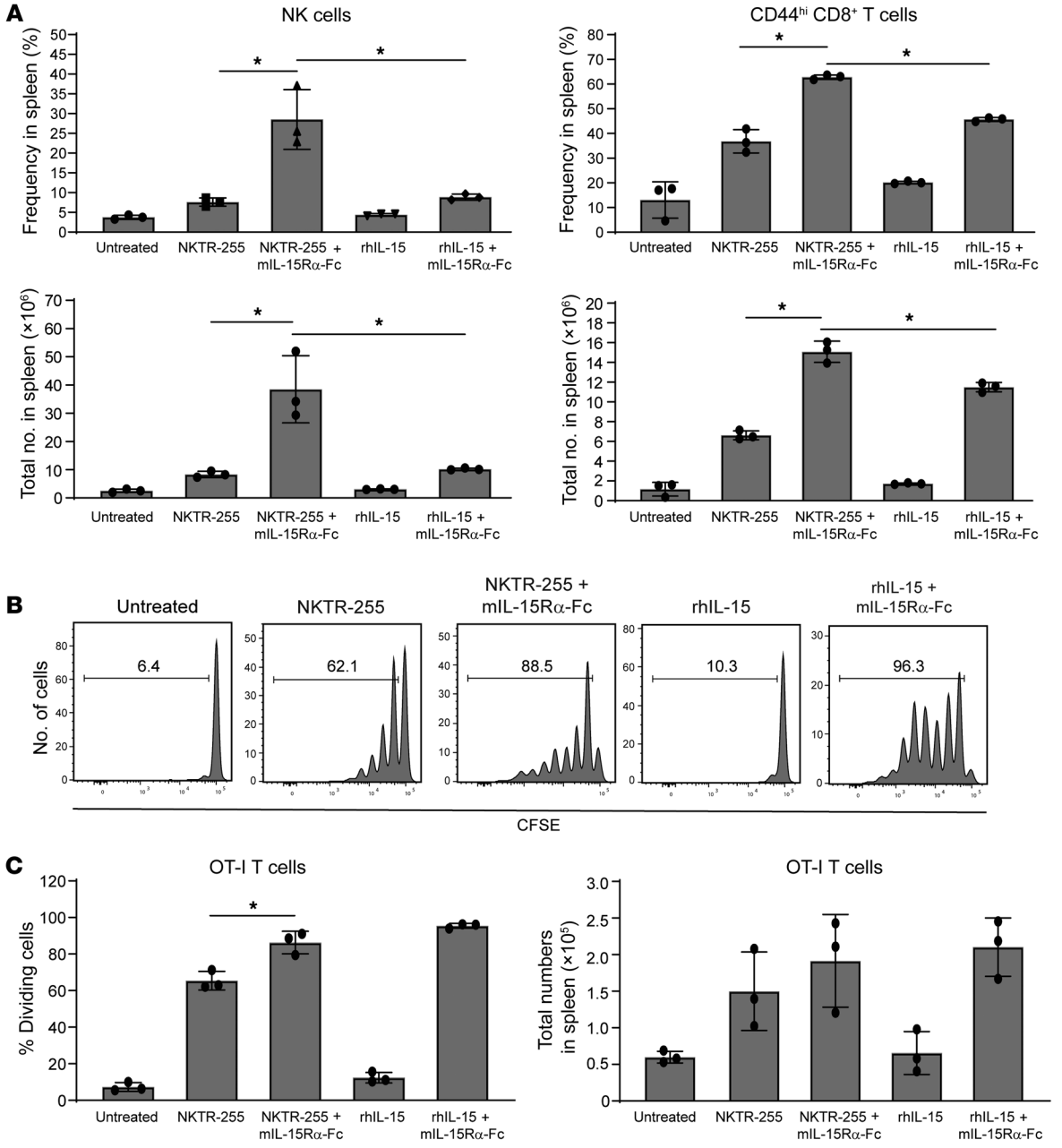

Figure 8. NKTR-255 and rhIL-15 form agonistic complexes with rmIL-15Rα-Fc. WT mice containing CFSE-labeled naive OT-I T cells (CD45.1+) were treated i.p. with NKTR-255 (0.6 μg), precomplexed NKTR-255/mIL-15Rα-Fc (0.6 μg/3.6 μg), rhIL-15 (0.6 μg), or precomplexed rhIL-15/mIL-15Rα-Fc (0.6 μg/3.6 μg). NKTR-255 and rhIL-15 were mixed with mIL-15Rα-Fc 30 minutes prior to injection. Mice were analyzed 7 days later. (**A**) Average frequency of NK cells and CD44hi CD8+ T cells in spleens (top row) and total numbers of the indicated lymphocyte populations in spleens (bottom row). (**B**) Representative CFSE dilution of CD45.1+ OT-I T cells. (**C**) Average frequency of dividing OT-I T cells and total numbers of OT-I T cells in spleens of treated mice (n = 3 mice/group). Error bars represent SD. *P < 0.05, 1-way ANOVA and 2-tailed Student's t test. Similar results were observed in at least 2 additional experiments.

more potent than rhIL-15/rmIL-15Rα–Fc in stimulating NK cells (Figure 8A). This result indicated that converting NKTR-255 from an IL-15Rαβ agonist to an IL-15Rβ agonist may skew the response toward NK cells.

Previous studies have reported that rhIL-15Rα–Fc is antagonistic to rhIL-15 while rmIL-15Rα–Fc is agonistic in vitro (18, 27, 28). To determine whether rhIL-15Rα–Fc is antagonistic or agonistic for NKTR-255, uncomplexed NKTR-255 or NKTR-255 precomplexed with rhIL-15Rα–Fc was given to mice containing CFSE-labeled naive OT-I T cells. Since both rmIL-15Rα–Fc and rhIL-15Rα–Fc were engineered with the same Fc fragment, any differences observed were not due to differences in Fc binding. As before, NKTR-255 increased expansion of OT-I T cells, CD44hi CD8+ T cells, and NK cells (Figure 9). In contrast NKTR-255 complexed with rhIL-15Rα-Fc had little effect on all 3 lymphocyte populations (Figure 9). These findings demonstrated that rhIL-15Rα–Fc antagonized NKTR-255 in a manner similar to that which has been observed with rhIL-15.

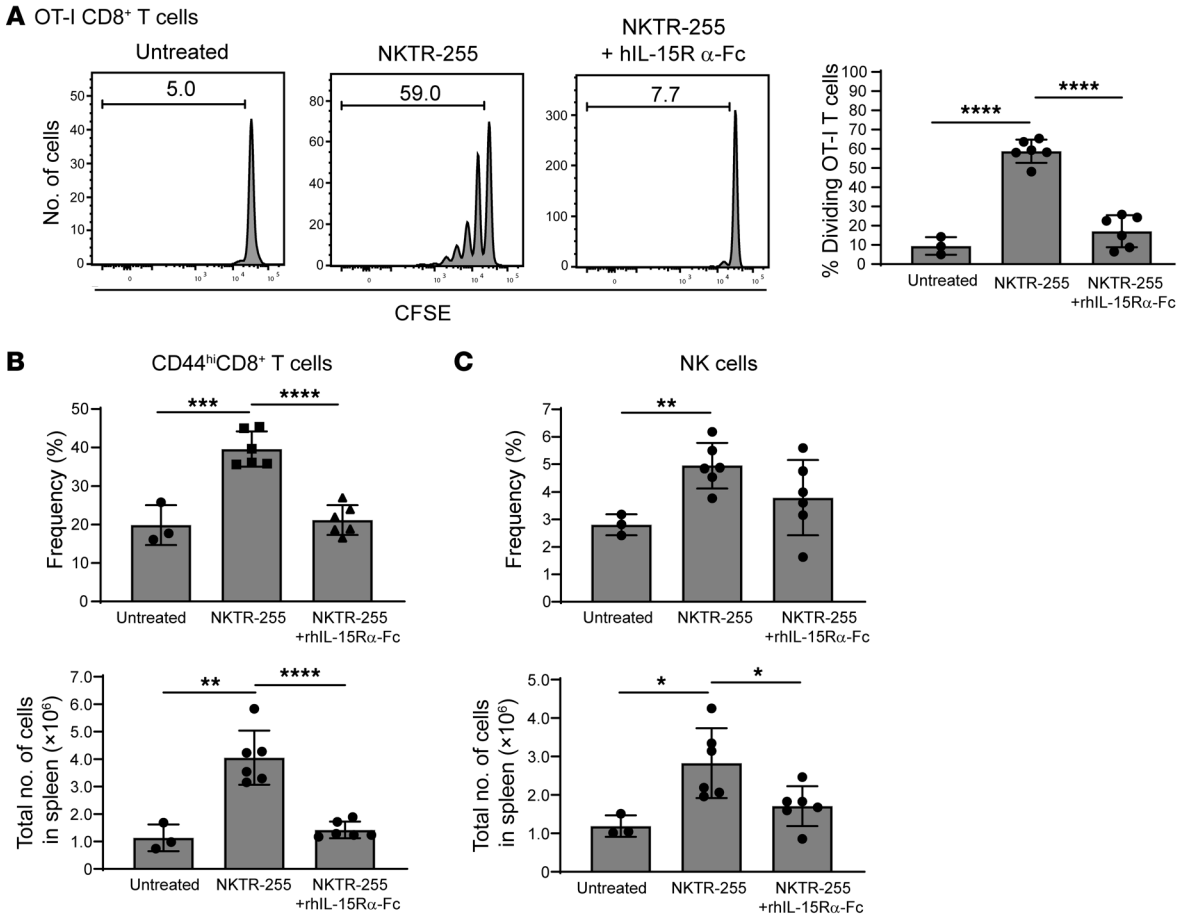

Figure 9. NKTR-255 forms antagonist complexes with rhIL-15Rα-Fc. Naive OT-I T cells (CD45.1+) were CFSE labeled and transferred into CD45.2+ WT mice (n = 3–6 mice/group). One day later, mice were treated i.p. with either NKTR-255 (0.6 μg) or precomplexed NKTR-255/rhIL-15Rα-Fc (0.6 μg/3.6 μg). Mice were analyzed 7 days later. (**A**) Representative CFSE dilution of OT-I T cells. (**B** and **C**) Average frequency and total number of CD44hiCD8+ T cells and NK cells in spleens. Error bars represent SD. *P < 0.05; **P < 0.01; ***P < 0.001; ****P < 0.0001, 1-way ANOVA and 2-tailed Student's t test.

Discussion

There have been numerous attempts to generate IL-15 agonists with an increased in vivo half-life and/or increased potency. Previous attempts have mostly combined IL-15 with a soluble version of IL-15Rα (8). These agents act as IL-2/IL-15β chain agonists independently of cellular expression of either IL-2Rα or IL-15Rα. Therefore, sIL-15 complexes preferentially stimulate lymphocytes with the highest expression of IL-2/IL-15Rβ, including NK cells, memory phenotype CD8+ T cells, and to a lesser extent, naive CD8+ T cells. Such cellular targeting is designed to enhance antitumor responses, as these cell types are integral in mediating tumor-specific killing. In developing NKTR-255, Nektar utilized polymer conjugation to generate an IL-15R agonist with enhanced in vivo PK compared with native IL-15 (29). Polymer conjugation produces an IL-15R agonist with an increased in vivo half-life that induces responses similar to those of sIL-15 complexes at a fraction of the dose and with no overt toxicities (22). In our study, we show that, in addition to having beneficial in vivo pharmacokinetics, NKTR-255 also possesses unique mechanisms of action.

Because IL-15Rα has a very high affinity for IL-15 and is expressed by CD8+ T cells and NK cells, it was integral to our studies to elucidate the role of IL-15Rα on NKTR-255 responses. While we originally hypothesized that NKTR-255 would employ trans presentation as a mechanism similar to that of IL-15, we discovered that IL-15Rα expression by opposing cells was irrelevant to NKTR-255 activity, indicating that NKTR-255 acts in a different manner than either rhIL-15 or endogenously expressed IL-15. However, since NKTR-255 responses were absent in IL-15Rα$^{-/-}$ mice and we could observe NKTR-255 binding to IL-15Rα, the presence of IL-15Rα was also likely important. This suggested that NKTR-255 was either cis presented or formed complexes with sIL-15Rα to generate IL-15Rα–dependent cytokines. Cis presentation is a mechanism whereby NKTR-255 binds IL-15Rα expressed by lymphocytes that facilitates binding to an adjacent IL-2/IL-15Rβγ$_C$ complex. Indeed, we found evidence that NKTR-255 uses cis presentation and forms complexes with sIL-15Rα.

By examining defined lymphocyte populations that lacked IL-15Rα, we found that responses to NKTR-255 by IL-15Rα$^{-/-}$ naive or memory CD8+ T cells were impaired. The responses to NKTR-255 by IL-15Rα$^{-/-}$ memory CD8+ T cells were not completely abrogated, demonstrating that NKTR-255 had some affinity for the IL-2/IL-15Rβγ$_C$ complex. Overall, memory CD8+ T cells were less dependent on IL-15Rα than naive CD8+ T cells, which correlated with their increased IL-2/IL-15Rβ expression (23).

Interestingly, expression of IL-15Rα by NK cells was not required for responses to NKTR-255. Therefore, NKTR-255 acted as an IL-15Rαβ agonist on CD8$^+$ T cells, unlike sIL-15 complexes that act solely as IL-15Rβ agonists. We suspect that NKTR-255 acted as an IL-15Rβ agonist on NK cells because NK cells express higher levels of IL-15Rβ and lower levels of IL-15Rα than memory CD8$^+$ T cells. Memory CD8$^+$ T cells also express higher levels of IL-15Rβ than naive CD8$^+$ T cells (26) and are less dependent on IL-15Rα for NKTR-255 responses. Together, these findings demonstrate that IL-15Rβ expression inversely correlates with its dependence on IL-15Rα expression. This attribute provided an explanation for why NKTR-255 was stimulatory at such low doses and why memory CD8$^+$ T cell responses were more robust than those of NK cells. This appeared to contrast with sIL-15 complexes (i.e., IL-2/IL-15β chain agonist molecules) that more potently stimulate NK cells over CD8$^+$ T cells (30).

We also investigated whether NKTR-255 formed soluble complexes with sIL-15Rα and whether these complexes were stimulatory or inhibitory. We utilized mice that lacked cell-surface IL-15Rα in the systemic lymphoid tissues, but had marked levels of sIL-15Rα. We found that mice with excess sIL-15Rα did not have enhanced responses to NKTR-255, but rather exhibited impaired responses. Our findings were in line with previous studies showing recombinant murine sIL-15Rα (containing no Fc) inhibits collagen-induced arthritis, delayed hypersensitivity, allergic-specific T cells, and allogenic and inflammatory responses (31–34). The high levels of sIL-15Rα present systemically in our mouse model may not reflect a physiological situation; however, it is possible that a specific tissue and tumor type may produce significant quantities in the local environment. While there is little information regarding the expression levels of sIL-15Rα or its regulation, there are reports that patients with head and neck tumors express increased levels of sIL-15Rα, where increased levels of sIL-15Rα correlated to poor clinical outcomes (24). We were unable to explain why the binding of NKTR-255 to sIL-15Rα was inhibitory and did not form agonistic complexes, when forming complexes prior to injection led to more robust responses. We suspect that the endogenously produced sIL-15Rα, when present in excess, competed with the cell-surface IL-15Rα expressed by the responding lymphocytes and the complexed NKTR-255/IL-15Rα.

We found it interesting that NKTR-255 formed a superagonist with rmIL-15Rα–Fc, but was antagonized by rhIL-15Rα–Fc. Since such antagonistic behavior was previously observed with rhIL-15 (18, 27, 28), the antagonism by rhIL-15Rα–Fc did not appear to be a unique attribute of NKTR-255 when compared with rhIL-15, and thus this property of rhIL-15 was not altered by the PEGylation approach employed for NKTR-255. Using different IL-15Rα mutants, Bouchaud et al. (35) made the observation that the antagonist properties of rhIL-15Rα were due to a 13–amino acid peptide region adjacent to the cytokine-binding domain that created a steric constraint impeding the binding of sIL-15Rα–IL-15 complexes to membrane-anchored IL-15Rαβγ. More importantly, the ability for soluble rhIL-15Rα to inhibit IL-15 and NKTR-255 suggested that the expression level of endogenous sIL-15Rα in patients may potentially affect responses to NKTR-255. Hence, further investigations examining human lymphocyte responses to NKTR-255 are warranted to validate our findings in mice. Overall, our findings examining NKTR-255 responses in mice are likely relevant to patients, as human lymphocytes have a similar hierarchy of IL-15 responsiveness among NK cells and CD8$^+$ T cells. An exception pertains to CD4$^+$ T cells, where human CD4$^+$ T cells are somewhat responsive to IL-15 while mouse CD4$^+$ T cells are poorly responsive. Therefore, human CD4$^+$ T cells should respond to NKTR-255, albeit still to a lesser extent than CD8$^+$ T cells. Our ability to visualize effects of NKTR-255 on purified CD8$^+$ T cell populations and perform fate analysis highlighted one advantage of using mouse models. Studies that rely solely on examining changes in bulk lymphocyte populations cannot determine how alterations in cell phenotypes affect the readout in changing lymphocyte populations.

This study elucidates unique attributes of NKTR-255, including its associated mechanisms of action and the impact of polymer conjugation of IL-15. For CD8$^+$ T cells, NKTR-255 acts as an IL-15Rαβ agonist, demonstrating agonistic activity that translates to a wider activation of CD8$^+$ T cells and skewing responses more heavily toward memory CD8$^+$ T cells compared with IL-15Rβ agonists, as these cells express high levels of both IL-15Rα and IL-15Rβ. NKTR-255 is unique among other IL-15 agonists currently under clinical investigation that induce potent NK cell responses (36, 37). Interestingly, even though treatment with NKTR-255 leads to a greater increase in CD62L$^+$CD44^{hi} CD8$^+$ T cells than CD62L$^-$CD44^{hi} CD8$^+$ T cells, a similar increase is not observed with established antigen-specific memory CD8$^+$ T cells. Based on this finding, we conclude that the conversion of naive CD8$^+$ T cells to CD62L$^+$CD44^{hi} CD8$^+$ T cells in response to NKTR-255 stimulation contributes in part to the observed increase in this cell population. Finally, we provide evidence that NKTR-255, like rhIL-15, is subject to potential inhibition by sIL-15Rα. Therefore, in addition to recommending prescreening of patients for levels of sIL-15Rα prior to administering NKTR-255, further studies are recommended to provide a better understanding of the regulation of NKTR-255 by sIL-15Rα. Alternatively, treatment with rhIL-15Rα could be used as a strategy to stifle an exaggerated response to NKTR-255. Overall, these findings highlight the potential of NKTR-255 to modify IL-15Rα dependency, provide differentiated mechanisms of action on CD8$^+$ T cells and NK cells, and provide unique therapeutic benefits.

Methods

Mice. Female WT C57BL/6, CD45.1$^+$ C57BL/6, and BALB/c mice were purchased from the Charles River through the NCI program. IL-15Rα$^{-/-}$ mice (38) were originally generated and obtained by Averil Ma (Department of Medicine, UCSF, San Francisco, California, USA) through Leo Lefrancois (Department of Immunology, University of Connecticut, Farmington, Connecticut, USA) and backcrossed to the C57BL/6 line. Villin–IL-15Rα Tg mice (IL-15Rα$^{-/-}$) (26) were backcrossed to the C57BL/6 background. CD45.1$^+$ OT-I TCR Tg mice on the RAG$^{-/-}$ background were originally provided by Leo Lefrancois or James P. Allison (University of Texas MD Anderson Cancer Center) and bred in house. OT-I TCR Tg mice were also crossed to the IL-15Rα$^{-/-}$ background and maintained as RAG$^{-/-}$ CD45.1$^+$CD45.2$^+$. All Tg and gene-deficient mice were completely backcrossed to the C57BL/6 background (at least 10 times). All mice were maintained under specific pathogen–free conditions at the University of Texas MD Anderson Cancer Center.

Generation of BM chimeras. BM cells were obtained from the tibia and femurs of IL-15Rα$^{-/-}$ (CD45.2$^+$) and WT (CD45.2$^+$) mice and depleted of T cells as previously described (39). WT (CD45.1$^+$) recipients were irradiated with 10 Gy and injected i.v. with 5×10^6 BM cells. BM reconstitution was confirmed 12 weeks later by analysis of BM-derived cells (CD45.2$^+$) in the peripheral blood.

Treatment with NKTR-255 and sIL-15 complexes. NKTR-255 was provided by Nektar Therapeutics. Mice were administered NKTR-255 at a concentration of 0.03 mg/kg in 200 μL of PBS via i.p. injection.

The rhIL-15 was provided by Nektar Therapeutics, while rmIL-15 was purchased from PeproTech. Mice were administered 4 doses of rhIL-15 (5 μg) in 200 μL of PBS by i.p. injection every 2 days. rmIL-15Rα–Fc and rhIL-15Rα–Fc were purchased from R&D Systems. Mice were administered precomplexed rhIL-15/sIL-15Rα–Fc (0.5 μg/3 μg) in 200 μL of PBS i.p.

Lymphocyte isolation and flow cytometry. Spleens and LNs were homogenized in HBSS containing Hepes, L-glutamine, penicillin/streptomycin, and gentamicin sulfate (HGPG) (HBSS/HGPG) using frosted slides. RBCs were lysed with Tris-ammonium chloride. All cells were filtered through a 70 μm nitex membrane before staining. For flow cytometric analysis, cells were stained in 1× PBS containing 0.2% BSA and 0.1% NaN_3 with appropriately diluted Abs at 4°C for at least 20 minutes. The following mAbs were purchased from BD Biosciences, eBioscience, BioLegend, or Tonbo Biosciences: CD45.1 (clone A20, BioLegend), CD45.2 (clone 104, BD), CD4 (GK1.5, Tonbo), CD8α (clone 53-6.7, Tonbo), CD44 (clone IM7, BD), CD62L (clone MEL-14, BioLegend), NK1.1 (clone PK136, BD), NKp46 (clone 29A1.4, BD), and CD11c (clone HL-3, BioLegend). To measure BrdU incorporation, mice were treated with 1 dose of NKTR-255 (0.03 mg/kg i.p.) or PBS followed by i.p. administration of BrdU (2 mg; Sigma-Aldrich). Administration of BrdU was repeated every 2 days. BrdU incorporation was detected by staining using the BrdU Flow Kit (catalog 559619) according to the manufacturer's instructions (BD Biosciences) following cell-surface staining. Flow cytometric data were acquired using LSR Fortessa (BD Biosciences) and analyzed with FlowJo software, version 10.

For detection of cell-surface binding of NKTR-255, WT, IL-15Rα$^{-/-}$, and CD11c-IL-15Rα Tg mice were sacrificed 24 hours after treatment with NKTR-225 (0.3 mg/kg, i.p.) or no treatment. Single-cell suspensions were incubated with APC-conjugated anti–hIL-15 Abs (catalog IC2471A, R&D Systems) for 15 minutes, washed, and then stained for additional cell-surface markers as previously described. For detection of NKTR-255 binding in vitro, isolated splenocytes from untreated mice were incubated with NKTR-255 or rmIL-15 for 15 minutes, washed, and stained with APC-conjugated anti–hIL-15 Ab followed by cell-surface staining as before.

Detection of sIL-15Rα. ELISAs specific for murine sIL-15Rα (R&D Systems) were performed according to the manufacturer's recommendations. For serum isolation, peripheral blood was collected from sacrificed mice via cardiac puncture and occasionally from the retro-orbital cavity. Blood was allowed to clot and centrifuged to separate serum.

Adoptive transfer. LNs from CD45.1$^+$ OT-I TCR Tg mice (RAG$^{-/-}$) were homogenized in HBSS/HGPG-yielding cells that included more than 95% TCRVα2$^+$CD8α$^+$ T cells. LN cells were incubated for 9 minutes at 37°C with CFSE (8 μM; Molecular Probes), and the reaction was squelched with HBSS supplemented with 5% FCS. CFSE-labeled cells were resuspended in PBS and injected i.v. into CD45.2$^+$ recipient mice (~1×10^6 OT-I T cells/mouse). One day after transfer, recipient mice were administered 1 dose of NKTR-255 at a concentration of 0.03 mg/kg or 0.6 μg/mouse in 200 μL of PBS i.p. Between 5 and 7 days after NKTR-255 injection, lymphocytes in the spleen were analyzed for the presence of OT-I donor cells (CD45.1$^+$) and CFSE dilution. For combination experiments, spleen and LN cells from CD45.1$^+$ WT and CD45.1$^+$CD45.2$^+$ IL-15Rα$^{-/-}$ OT-I mice were mixed at a 1:1 ratio, CSFE labeled, and adoptively transferred into CD45.2$^+$ recipient mice. One day after transfer, recipient mice were administered 1 dose of NKTR-255 (0.03 mg/kg, i.p.). Around 1 week later, after treatment with NKTR-255, CFSE dilution of donor cells in pLNs and spleens was analyzed.

To generate memory CD8$^+$ T cells, CD45.1$^+$ WT or IL-15Rα$^{-/-}$ OT-I TCR Tg T cells were adoptively transferred (i.v.) into C57BL/6 mice and infected with VSV-OVA (Indiana serotype) 1 day later. Thirty-five days after infection, spleen cells were negatively enriched (yielding ~ 85% CD8α$^+$ T cell purity) using the Dynal CD8 Enrichment Kit (Invitrogen), CFSE labeled, and injected i.v. into CD45.2$^+$ WT or IL-15Rα$^{-/-}$ recipients (between 4 and 6×10^6 CD8$^+$ T cells/mouse). Memory OT-I T cells made up approximately 10% of the CD8$^+$ T cells. Recipient mice were administered 1 dose of NKTR-255 (0.03 mg/kg, i.p.) 1 day after transfer and analyzed for the presence of CD45.1$^+$ OT-I donor cells and CFSE dilution 1 week later.

Statistics. Graphical presentation and statistical analysis of the data were performed using GraphPad Prism, version 7 (GraphPad Software) or Microsoft Excel 2010. Data are represented as mean ± SD. Results between experimental groups were compared using 2-tailed Student's *t* test and 1-way ANOVA. $P < 0.05$ was considered statistically significant. Statistical significance is shown as follows: $^*P < 0.05$; $^{**}P < 0.01$; $^{***}P < 0.001$; $^{****}P < 0.00001$.

Study approval. All animal procedures were conducted on mice between 6 and 10 weeks of age in accordance with the animal care and use protocols (00000851-RN02) approved by the IACUC at the University of Texas MD Anderson Cancer Center. The animal facility was fully accredited by the Association of Assessment and Accreditation of Laboratory Animal Care International.

Author contributions

KSS defined the research theme, guided the research, analyzed data, interpreted data, and wrote the paper. TOR performed experiments, analyzed data, and wrote the paper. SMH, AC, AG, and SR performed experiments and analyzed data. LM, JZ, and TM interpreted data.

Acknowledgments

This research was supported by Nektar Therapeutics (to KSS) and by the MD Anderson Cancer Center–Cancer Center Prevention Research Institute of Texas (CPRIT) Summer Research Program (to AJC). Editorial assistance was provided by BOLDSCIENCE Ltd. and funded by Nektar Therapeutics.

Address correspondence to: Kimberly S. Schluns, Kite Pharma, 2400 Broadway, Santa Monica, California 90404, USA. Phone: 310.824.9999; Email: kschluns@kitepharma.com.

KSS's present address is: Kite Pharma, Santa Monica, California, USA.

1. Schluns KS, et al. Cutting edge: requirement for IL-15 in the generation of primary and memory antigen-specific CD8+ T cells. *J Immunol*. 2002;168(10):4827–4831.
2. Becker TC, et al. Interleukin 15 is required for proliferative renewal of virus-specific memory CD8+ T cells. *J Exp Med*. 2002;195(12):1541–1548.
3. Ranson T, et al. IL-15 is an essential mediator of peripheral NK-cell homeostasis. *Blood*. 2003;101(12):4887–4893.
4. Kanegane H, Tosato G. Activation of naive and memory T cells by interleukin-15. *Blood*. 1996;88(1):230–235.
5. Richer MJ, et al. Inflammatory IL-15 is required for optimal memory T cell responses. *J Clin Invest*. 2015;125(9):3477–3490.
6. Tamang DL, et al. Induction of granzyme B and T cell cytotoxic capacity by IL-2 or IL-15 without antigens: multiclonal responses that are extremely lytic if triggered and short-lived after cytokine withdrawal. *Cytokine*. 2006;36(3–4):148–159.
7. Borger P, et al. Interleukin-15 differentially enhances the expression of interferon-gamma and interleukin-4 in activated human (CD4+) T lymphocytes. *Immunology*. 1999;96(2):207–214.
8. Robinson TO, Schluns KS. The potential and promise of IL-15 in immuno-oncogenic therapies. *Immunol Lett*. 2017;190:159–168.
9. Waldmann TA. The biology of interleukin-2 and interleukin-15: implications for cancer therapy and vaccine design. *Nat Rev Immunol*. 2006;6(8):595–601.
10. Dubois S, et al. IL-15Ralpha recycles and presents IL-15 in trans to neighboring cells. *Immunity*. 2002;17(5):537–547.
11. Bergamaschi C, et al. Circulating IL-15 exists as heterodimeric complex with soluble IL-15Rα in human and mouse serum. *Blood*. 2012;120(1):e1–e8.
12. Giri JG, et al. Identification and cloning of a novel IL-15 binding protein that is structurally related to the alpha chain of the IL-2 receptor. *EMBO J*. 1995;14(15):3654–3663.
13. Anderson DM, et al. Functional characterization of the human interleukin-15 receptor alpha chain and close linkage of IL15RA and IL2RA genes. *J Biol Chem*. 1995;270(50):29862–29869.
14. Stonier SW, et al. Dendritic cells drive memory CD8 T-cell homeostasis via IL-15 transpresentation. *Blood*. 2008;112(12):4546–4554.
15. Stonier SW, Schluns KS. Trans-presentation: a novel mechanism regulating IL-15 delivery and responses. *Immunol Lett*. 2010;127(2):85–92.
16. Anthony SM, et al. Soluble interleukin-15 complexes are generated in vivo by type I interferon dependent and independent pathways. *PLoS One*. 2015;10(3):e0120274.
17. Anthony SM, Schluns KS. Emerging roles for IL-15 in the activation and function of T-cells during immune stimulation. *Res Rep Biol*. 2015;6:25–37.
18. Mortier E, et al. Natural, proteolytic release of a soluble form of human IL-15 receptor alpha-chain that behaves as a specific, high affinity IL-15 antagonist. *J Immunol*. 2004;173(3):1681–1688.
19. Hayakawa Y, Smyth MJ. CD27 dissects mature NK cells into two subsets with distinct responsiveness and migratory capacity. *J Immunol*. 2006;176(3):1517–1524.
20. Ekladious I, et al. Polymer-drug conjugate therapeutics: advances, insights and prospects. *Nat Rev Drug Discov*. 2019;18(4):273–294.
21. Overwijk WW, et al. Engineering IL-2 to give new life to T cell immunotherapy. *Annul Rev Med*. 2021;72(1):281–311.
22. Miyazaki T, et al. NKTR-255, a novel polymer-conjugated rhIL-15 with potent antitumor efficacy. *J Immunother Cancer*. 2021;9(5):e002024.
23. Zhang X, et al. Potent and selective stimulation of memory-phenotype CD8+ T cells in vivo by IL-15. *Immunity*. 1998;8(5):591–599.
24. Badoual C, et al. The soluble alpha chain of interleukin-15 receptor: a proinflammatory molecule associated with tumor progression in head and neck cancer. *Cancer Res*. 2008;68(10):3907–3914.
25. Santana Carrero RM, et al. IL-15 is a component of the inflammatory milieu in the tumor microenvironment promoting antitumor responses. *Proc Natl Acad Sci U S A*. 2019;116(2):599–608.
26. Ma LJ, et al. Trans-presentation of IL-15 by intestinal epithelial cells drives development of CD8alphaalpha IELs. *J Immunol*. 2009;183(2):1044–1054.
27. Stoklasek TA, et al. Combined IL-15/IL-15Ralpha immunotherapy maximizes IL-15 activity in vivo. *J Immunol*. 2006;177(9):6072–6080.
28. Rubinstein MP, et al. Converting IL-15 to a superagonist by binding to soluble IL-15R{alpha}. *Proc Natl Acad Sci U S A*. 2006;103(24):9166–9171.
29. Kirk P, et al. NKTR-255: an IL-15-based therapeutic with optimized biological activity and anti-tumor efficacy. https://www.nektar.com/application/files/5314/7887/7645/2016_SITC_NKTR-255-preclinical_poster.pdf. Accessed August 9, 2021.
30. Knudson KM, et al. Rationale for IL-15 superagonists in cancer immunotherapy. *Expert Opin Biol Ther*. 2020;20(7):705–709.
31. Ruchatz H, et al. Soluble IL-15 receptor alpha-chain administration prevents murine collagen-induced arthritis: a role for IL-15 in development of antigen-induced immunopathology. *J Immunol*. 1998;160(11):5654–5660.
32. Rückert R, et al. Dendritic cell-derived IL-15 controls the induction of CD8+ T cell immune responses. *Eur J Immunol*. 2003;33(12):3493–3503.
33. Rückert R, et al. Blocking IL-15 prevents the induction of allergen-specific T cells and allergic inflammation in vivo. *J Immunol*. 2005;174(9):5507–5515.
34. Wei X, et al. The Sushi domain of soluble IL-15 receptor alpha is essential for binding IL-15 and inhibiting inflammatory and allogenic responses in vitro and in vivo. *J Immunol*. 2001;167(1):277–282.
35. Bouchaud G, et al. The exon-3-encoded domain of IL-15ralpha contributes to IL-15 high-affinity binding and is crucial for the IL-15 antagonistic effect of soluble IL-15Ralpha. *J Mol Biol*. 2008;382(1):1–12.
36. Kim PS, et al. IL-15 superagonist/IL-15RαSushi-Fc fusion complex (IL-15SA/IL-15RαSu-Fc; ALT-803) markedly enhances specific subpopulations of NK and memory CD8+ T cells, and mediates potent anti-tumor activity against murine breast and colon carcinomas. *Oncotarget*. 2016;7(13):16130–16145.
37. Margolin K, et al. Phase I trial of ALT-803, a novel recombinant IL15 complex, in patients with advanced solid tumors. *Clin Cancer Res*. 2018;24(22):5552–5561.
38. Lodolce JP, et al. IL-15 receptor maintains lymphoid homeostasis by supporting lymphocyte homing and proliferation. *Immunity*. 1998;9(5):669–676.
39. Castillo EF, et al. Dendritic cells support the in vivo development and maintenance of NK cells via IL-15 trans-presentation. *J Immunol*. 2009;183(8):4948–4956.